

Plant production of high affinity nanobodies that block SARS-CoV-2 spike protein binding with its receptor, human angiotensin converting enzyme

1 Marco Pitino¹, Laura A. Fleites¹, Lauren Shrum¹, Michelle Heck², Robert G. Shatters, Jr.^{3,*}

2 ¹AgroSource, Inc., Jupiter, FL, USA

3 ²Emerging Pests and Pathogens Research Unit, USDA Agricultural Research Service, Ithaca, NY,
4 USA

5 ³U.S. Horticultural Research Laboratory, Unit of Subtropical Insects and Horticulture, USDA
6 Agricultural Research Service, Fort Pierce, FL, USA

7 * Correspondence:

8 Robert G. Shatters, Jr.

9 Robert.Shatters@USDA.gov

10 **Keywords:** SARS-CoV-2, nanobody, plant, V_{HH}, competitive ELISA, ACE2 (Min.5-Max. 8)

11 Abstract

12 Nanobodies® (V_{HH} antibodies), are small peptides that represent the antigen binding domain, V_{HH} of
13 unique single domain antibodies (heavy chain only antibodies, HcAb) derived from camelids. Here,
14 we demonstrate production of V_{HH} nanobodies against the SARS-CoV-2 spike proteins in the
15 solanaceous plant *Nicotiana benthamiana* through transient expression and their subsequent detection
16 verified through western blot. We demonstrate that these nanobodies competitively inhibit binding
17 between the SARS-CoV-2 spike protein receptor binding domain and its human receptor protein,
18 angiotensin converting enzyme 2 (ACE2). We present plant production of nanobodies as an
19 economical and scalable alternative to rapidly respond to therapeutic needs for emerging pathogens
20 in human medicine and agriculture.

21 0 Introduction

22 Severe acute respiratory syndrome coronavirus 2 (SARS-CoV-2) is a member of the subfamily
23 *Coronaviridae* in the family *Coronaviridae* and the order *Nidovirales*. Pathogenic viruses in this
24 subfamily cause severe respiratory syndrome in humans. SARS-CoV-2 is related to SARS-CoV-1
25 and Middle Eastern Respiratory Syndrome (MERS-CoV), which emerged in humans in 2003 and
26 2012, respectively. SARS-CoV-2 is responsible for the 2019 pandemic and COVID-19 disease
27 (Huang, Wang et al. 2020). COVID-19 disease results in a range of outcomes, ranging from
28 asymptomatic infection to patient death. To date, global vaccinations for SARS-CoV-2 protections
29 are underway, but additional treatments are needed to prevent infection among naïve and even
30 vaccinated individuals. Tiered prevention efforts have been shown to reduce transmission and
31 severity of disease outcome.

32
33 Coronaviruses are positive-sense, single-stranded RNA viruses with spherical virions bound by a
34 membrane envelope that are 100-160nm in diameter. The 3' end of the viral genome encodes the

35 structural proteins, including the envelop glycoprotein spike (S), envelop (E), membrane (M) and
36 nucleocapsid (N). Inserted into the membrane envelop are ~25 copies of the homotrimeric
37 transmembrane spike glycoprotein (spike protein) as a clover-shaped trimer, with three S1 heads and
38 a trimeric S2 stalk (Benton, Wrobel et al. 2020). The receptor binding domain (RBD) is situated atop
39 each S1 head (Nishima and Kulik 2021). The RBD is responsible for entry into host cells (Wang,
40 Zhang et al. 2020, Jackson, Farzan et al. 2022) via interaction with the protein angiotensin converting
41 enzyme 2 (ACE2), the interaction which also determines the viral host range (Yan, Zhang et al.
42 2020). Studies have shown a higher affinity for SARS-CoV-2 to ACE2 as compared to ACE1,
43 further supporting its role in transmission and virulence (Samavati and Uhal 2020). Highly
44 transmissible viral variants, such as Delta and Omicron variant, have been selected for during the
45 pandemic and exhibit mutations in the RBD (Li, Lai et al. 2021) (Saxena, Kumar et al. 2022). Thus,
46 interactions between ACE2 and the RBD are attractive targets for the development of novel anti-viral
47 therapies.

48
49 Nanobodies represent a promising new therapy for the treatment of viral diseases, including COVID-
50 19. A pubmed search for SARS-CoV-2 and nanobody brings up a total of 21 peer-reviewed
51 publications (Esparza, Martin et al. 2020). Nanobodies, also referred to as V_{HH}, are produced by
52 animals in the camelid family, which include llamas and alpacas. Coined by the popular press as
53 mini-antibodies (Deyev and Lebedenko 2009), these IgGs are less than 15 kDa and are comprised of
54 an unpaired heavy-chain variable domain. Nanobodies have been reported to bind antigens with
55 affinities equivalent to a conventional IgG (Gonzalez-Sapienza, Rossotti et al. 2017, Asaadi,
56 Jouneghani et al. 2021). Nanobodies are also under development for the control of at least two crop
57 diseases: grapevine fanleaf virus in cultivated wine grapes (Yan, Zhang et al. 2020), botrytis, and
58 detection against a range of other plant pathogens (Njeru and Kusolwa 2021).

59
60 These antigen-binding proteins, derived from single-chain camelid antibodies, are significantly
61 smaller in size compared to conventional antibodies with a molecular mass of 12-15 kDa
62 (conventional antibodies are ~150 kDa). Key features of nanobodies that make them attractive
63 alternatives to conventional antibodies include their high affinity, specificity, solubility,
64 thermostability and mobility. Production of nanobodies is typically done by expression of the gene in
65 *E.coli*; however, a potentially more effective method is currently being studied based on plant
66 expression.

67
68 We represent a team of agricultural scientists developing sustainable and biologically-based solutions
69 to pathogens of economic importance in crop production. As part of this research, we developed a
70 low-cost, plant-based method of producing proteins that could be used to solve agricultural pathogen
71 problems in agricultural production settings. As a proof-of-concept, we describe the production of a
72 RBD nanobody in a plant expression system. The benefits of producing therapeutics in plants justify
73 considering plants to mass produce COVID-19 protein-based therapies.

74 **1 Materials and Methods**

75 **1.1 Construct Design**

76 A total of four constructs were designed for experimentation with plant expression of COVID-19
77 nanobodies. The methionine start codon of the SARS-CoV2 nanobody protein sequence (NIH-
78 CoVnb-112; Esparza et al. 2020) was removed and replaced with an N-terminal signal peptide
79 sequence for protein secretion into the apoplast and a 6x histidine tag at the C-terminus (SP-
80 CoV19_his). An analogous negative mutated control construct was also designed, such that the

81 amino acids spanning the three complementarity determining regions (CDR1, CDR2, CDR3) of the
82 native SARS-CoV2 nanobody sequence were scrambled using a random number generator SP-
83 *mCov19_his*; (Fig. S1). Disruption of the CDR regions was expected to abolish the interaction with
84 the receptor binding domain of the viral spike protein.

85 Two more variants of the SARS-CoV2 nanobody construct were made as fusions to monomeric
86 enhanced green fluorescent protein coding sequence (EGFP): one with an N-terminal 6x histidine tag
87 (SP-his_CoV19-GFP), and a second with a C-terminal 6x histidine tag (SP-CoV19_his-GFP; (Fig.
88 S1). This module was followed in both constructs by EGFP, with a P2A site (ribosome skipping
89 sequence allowing both CoV19-variants and EGFP to be produced as separate proteins) inserted
90 between the nanobody module and EGFP sequence. All constructs were codon-optimized for
91 expression in the Solanaceae using an online tool provided by Integrated DNA Technologies (IDT,
92 Illinois, USA; <https://www.idtdna.com/CodonOpt>) prior to uploading to the online ordering portal for
93 Codex DNA (La Jolla, CA). A 40bp span of nucleotide sequence homologous to the recipient vector
94 pNANO was added to the 5' and 3' ends of the constructs to enable cloning with the BioXP 3250
95 system (Codex DNA, La Jolla, CA).

96

97 **1.2 Construct Generation and Bacterial Transformation**

98 The plasmid backbone was linearized by sequential digestion with *SmaI* and *SpeI* (New England
99 Biolabs, Ipswich, MA, USA), and gel purified from 0.8% SeaPlaque GTG Agarose (Lonza,
100 Rockland, ME) using a phenol:chloroform:isoamyl alcohol extraction method followed by overnight
101 precipitation at -20°C in 100% ethanol, 0.3M NaOAc, pH 5.0. The purified, precipitated DNA was
102 washed with 70% ethanol, dried briefly, and resuspended in sterile nuclease free water. The final
103 constructs were generated in an overnight run on the BioXP 3250 system (Fig. 1A) (Codex DNA, La
104 Jolla, CA), an automated synthetic biology platform for DNA fragment assembly and cloning.

105 *Agrobacterium tumefaciens* EHA105 was electroporated with the BioXP products and grown on LB
106 supplemented with kanamycin (100µg/ml) for three days (Fig. 1B). Colonies were screened using
107 colony PCR and sequence verified prior to transient expression and purification in *N. benthamiana*.

108

109 **1.3 Plant Growth and Agroinfiltration**

110 *N. benthamiana* plants were grown under the greenhouse conditions and used at 4-5 weeks old for
111 transient expression using plant infiltration with *Agrobacterium* EHA105, which mechanically
112 delivers the bacteria to the plant's extracellular matrix (apoplast) (Kapila, De Rycke et al. 1997)
113 (Fig.1C). *Agrobacterium* EHA105 harboring pNANO plasmid was cultured overnight in 5 mL of LB
114 media with 100µg ml⁻¹ of kanamycin. Overnight culture was pelleted and resuspended in infiltration
115 buffer (10mM MgCl₂, 10mM MES, 400 µM acetosyringone) at optical density at 600 nm (OD₆₀₀)
116 0.3. For each construct, leaves were infiltrated with the bacterial suspension and set in greenhouse
117 for duration of experiment (Fig. 1C). Two days post infiltration (2 dpi), leaves were manually excised
118 from the plants using a sterile blade and processed for total protein extraction and purification.

119 **1.4 Protein Extraction and Purification**

120 *N. benthamiana* leaves were observed under UV light for GFP expression and harvested at 2 dpi
121 (days post infiltration) (Fig. 1D) followed by homogenization in liquid nitrogen. Total plant proteins
122 were extracted using native buffer (10mM Tris/HCl pH 7.5, 150mM NaCl, 0.5mM EDTA, 1% [v/v]
123 P9599 Protease Inhibitor Cocktail [Sigma-Aldrich], 1% [v/v] IGEPAL CA-630 [Sigma-Aldrich]). A
124 total of 5mL of extraction buffer per gram of leaf tissue was used. Samples were clarified by
125 centrifugation at 4°C at 3000 rcf. The supernatant was filtered through a 40 µm nylon cell strainer
126 (Becton Dickinson Labware, Franklin Lakes, NJ, US) and then used for purification process utilizing
127 Ni-NTA agarose columns (Thermo Scientific, Rockford, US), following manufacturers guidelines.
128 Briefly, imidazole binding buffer (20mM sodium phosphate, 10mM imidazole, 0.5mM NaCl, pH 7.4)
129 was used to equilibrate, bind, and wash the columns. To elute product of interest, (20mM sodium
130 phosphate, 500mM imidazole, 0.5mM NaCl, pH 7.4) was used.

131 **1.5 SDS-PAGE and Western Blotting**

132 Samples were denatured and reduced using 5x Lane Marker Reducing Sample Buffer (Thermo
133 Scientific, Rockford, IL, US), boiled at 95°C for 10 minutes, then stored on ice. Gradient 4-20%
134 precast polyacrylamide gels (Bio-Rad Laboratories, Hercules, CA) were loaded into electrophoresis
135 tank (Bio-Rad Laboratories) and filled with 1x Tris/Glycine/SDS buffer. Kaleidoscope ladder (Bio-
136 Rad Laboratories) was loaded into the first well (5µL), and each sample was loaded into every other
137 well. 25µL per sample were used for Coomassie staining, and 10µL per sample were used for
138 immunoblotting. Electrophoresis was run following manufacturing guidelines with a powerpack
139 (Bio-Rad Laboratories). One gel was stained with Coomassie blue, while the other gel was
140 transferred to a nitrocellulose membrane using the Trans-Blot Turbo Transfer system following
141 manufacturer guidelines (Bio-Rad Laboratories). The nitrocellulose membrane was removed and
142 placed in 1X Casein blocker for one hour on rotator followed by incubation with a 1:1000 dilution of
143 his HRP-conjugated antibodies (Proteintech, Rosemount, IL, US) for 1 hour room temperature. The
144 membrane was washed in 1X TBS three times in 10-minute intervals. ECL substrate (Bio-rad
145 Laboratories) that consists of 1 mL peroxide and 1mL luminol enhancer were spread onto membrane
146 and left for 5 minutes before observation using ChemiDoc imager (Bio-rad Laboratories).

147 **1.6 Competitive ELISA binding screen for ACE2 and RBD**

148 To verify the activity of recombinant nanobodies generated in plants, we conducted a competitive
149 binding assay that measures inhibition of the interaction between the receptor binding domain (RBD)
150 of the SARS-CoV-2 spike protein with the ACE2 receptor in the presence of the purified nanobodies.
151 Purified nanobodies were diluted at 1µg/mL and 0.1 µg/mL concentrations in association with RBD
152 proteins then added to the ACE2 coated plate (RayBiotech, Peachtree Corners, GA, US). Nanobodies
153 and RBD proteins were incubated at room temperature for one hour to allow interaction. The assay
154 plate was washed four times with a wash solution provided by ELISA kit (RayBiotech). HRP-
155 conjugated Anti-IgG was added to plate post wash and incubated at room temperature for one hour
156 with gentle shaking. After four additional washes, the plate was developed by addition of
157 tetramethylbenzidine and stopped after 30 minutes of gentle shaking in the dark with stop solution
158 (RayBiotech). Absorbency was measured immediately after adding stop solution at 450 nm on a plate
159 reader (Citation 1 imaging reader, BioTek, Winooski, VT, US).
160

161 **2 Results**

162 **2.1 Expression and purification of nanobodies for SARS-Cov-2 RBD in *N. benthamiana***

163 An initial test performed using SP-CoV19_his purified from transient expressing leaves showed an
164 expected ~15KDa band confirming expression and purification. This band was visualized by
165 Coomassie blue staining of an SDS-Page gel and western blot/immunodetection specific for the his-
166 tag on the SP-CoV19 protein (Fig. S2). Next, we tested SP-his_CoV19-GFP, SP-CoV19_his-GFP,
167 SP-*mCov19*_his sequences. GFP visualization of infiltrated leaves showed high levels of expression
168 two days post infiltration and leaves were harvested at this time and used for purification. Bands on
169 the Coomassie gel and western blot were visualized migrating between the 15 and 20 kDa marker
170 bands corresponding to the size of the SP-his_CoV19-GFP, SP-CoV19_his-GFP and SP-*mCov19*_his
171 sequences (Fig 2A,B).

172 **2.2 Biological activity of SARS-Cov-2 nanobody with ACE2 competition assay**

173 Next, we assessed the ability for plant produced nanobody to block ACE2 binding cells RBD
174 interaction. To evaluate relative inhibition of RBD protein from binding to ACE2 a competitive
175 ELISA inhibition assay was performed. RBD protein binding ACE2 was indicated by high
176 colorimetric absorbance. Initial screening was performed using SP-CoV19_his at 100,10,1 and 0.1
177 µg/mL concentrations (Fig. S2C). Competitive ELISA assay indicated that 1µg/mL SP-CoV19_his
178 inhibited interaction between ACE2 and RBD and was used for subsequent experiments. The same
179 results were obtained using both SP-his_CoV19-GFP and SP-CoV19_his-GFP, showing 100%
180 inhibition between ACE2 and RBD at 1µg/ml. Inhibition was also observed at 0.1µg/ml with 60-70%
181 inhibition (Fig. 3). In contrast, the mutated sequence SP-*mCov19*_his inhibited less than <20% at 1.0
182 µg/ml and 0% at 0.1 µg/ml (Fig. 3). These results showed that plant-produced SP-CoV19_his, SP-
183 his_CoV19-GFP and SP-CoV19_his-GFP, but not SP-*mCov19*_his, inhibit 100% ACE2 and RBD
184 interactions at 1µg/mL similarly to previous published data with NIH-CoVnb-112 production in yeast
185 system (Esparza et al. 2020).

186 **3 Discussion**

187 In this study, we provide proof of concept for in plant production of nanobodies that neutralize the
188 interaction between the human ACE2 receptor and the SARS-CoV-2 spike protein RBD, a key step
189 of the infection initiation process (Esparza, Martin et al. 2020). Binding inhibition was slightly
190 reduced with a 10-fold dilution of the nanobody, consistent with previous reports for the same
191 nanobody expressed in yeast (Esparza, Martin et al. 2020). Moreover, a modified nanobody with a
192 scrambled RBD binding domain failed to inhibit binding at the lower concentrations used,
193 demonstrating the binding specificity of the interaction between the plant-produced RBD-binding
194 nanobodies and the RBD. The plant expression constructs used two features to aid in nanobody
195 production: the use of a signal peptide targeting the nanobody to the plant apoplastic space and a self-
196 cleaving P2A peptide. A signal peptide was added for future nanobody production in plant cell tissue
197 culture systems, to support secretion of the nanobody through the cellular secretory pathway. The
198 self-cleaving P2A peptide enabled production of functional nanobodies with concurrent fluorescent
199 protein signal to monitor transient transformation events in *N. benthamiana* and to easily localize
200 regions of nanobody production *in planta*. Plant tissue was harvested at 2 days post-infiltration, and
201 thus not optimized for nanobody yield in this study. The His tag facilitated enrichment from the plant
202 proteome but would need to be removed prior to the development of plant-based nanobody therapies
203 for the treatment of human or other animal diseases. A recent example of production of RBD in
204 planta exhibits suitable biochemical and antigenic features for use in a subunit vaccine platform
205 (Demone, Nourimand et al. 2021). We posit that molecular farming of nanobodies, and other
206 biologicals is an under-developed area for cost savings and increased global access for the production
207 of protein and small molecule therapies.

208 Research using nanobodies in plants has been increasing rapidly in recent years (Dhama, Natesan et
209 al. 2020, Wang, Yuan et al. 2021), including in the development of therapies and diagnostic tools for
210 plant diseases. Plants offer several advantages for nanobodies expression over conventional
211 expression platforms including their easy transformation, low risk of pathogen contamination and
212 low cost for upscaling. In addition to injectable vaccines, new strategies are emerging and being
213 developed to increase protection against COVID-19, for example a nasal spray-delivered nanobody
214 offers a complementary barrier method to prevent virus acquisition into human epithelial cells in the
215 airway. Nanobodies are 12–15 kDa single-domain antibody fragments that can be delivered by
216 nebulizers and relatively easy and inexpensive to produce compared to other systems (Esparza et al.
217 2020). Previous cryo-electron microscopy studies showed SARS-CoV-2 spike protein and its
218 interaction with the cell receptor ACE2, such binding triggers a cascade of events that leads to the
219 fusion between cell and viral membranes for cell entry (Kirchdoerfer et al. 2018; Yuan et al. 2017;
220 Gui et al. 2017). Because SARS-CoV-2 binding spike protein RBD and the host ACE2 receptor
221 determines host susceptibility to the virus, interfering with that interaction might constitute a
222 treatment option (Walls et al. 2020). Esparza and colleagues (2020) showed that NIH-CoVnb-112
223 candidate nanobodies blocked interaction between ACE2 and RBD “wild type” and 3 variant forms,
224 also they showed that it retained structural integrity and potency after nebulization. A subset of these
225 nanobodies fold in planta and retain the structural features necessary to interfere with protein
226 interaction between ACE2 and the SARS-CoV-2 spike protein RBD. We demonstrate that
227 nanobodies produced in plants retain proper folding and functionality comparably to a yeast
228 production system supporting the use of plants as cost-effective production platforms for therapeutic
229 needs with emerging pathogens, such as the SARS-CoV-2 virus.

230 **4 Conflict of Interest**

231 The authors declare that the research was conducted in the absence of any commercial or financial
232 relationships that could be construed as a potential conflict of interest.

233 **5 Author Contributions**

234 MH, MP and RS conceived of the idea and provided grant funding. LF developed and constructed the
235 nanobody constructs. MP, LF and LS conducted the experiments. All authors contributed to data
236 analysis and writing and editing the paper.

237 **6 Funding**

238 Funding was provided by the U. S. Department of Agriculture CRIS project 8062-22410-007-000-D
239 and USDA, NIFA grant 2020-70029-33176.

240 **7 Acknowledgements**

241 We would like to thank Carrie Vanderspool and Mant Acon for the plants used in this study. Mention
242 of trade names or commercial products in this article is solely for the purpose of providing specific
243 information and does not imply recommendation or endorsement by the U.S. Department of
244 Agriculture.

245 **8 Supplementary Material**

246 Supplementary Material should be uploaded separately on submission, if there are Supplementary
247 Figures, please include the caption in the same file as the figure. Supplementary Material templates

248

249 **Figure 1. Schematic representation of workflow of production of nanobodies in plant system.**

250 A) Cloning with the BioXP 3250 Gibson Assembly[®]. B) Agrobacterium transformation. C)
251 Agrobacterium infiltration was performed by using 1 mL needleless syringes to inject bacteria into
252 the abaxial side of the leaves at OD₆₀₀ 0.3. D) P2A sequence was used for generating multiple
253 separate proteins from a single mRNA, GFP included in the sequence allowed prescreening of high
254 expression protein in leaves using UV light.

255

256 **Figure 2 – SDS PAGE and Western blot.** A) Coomassie blue stain was used to verify purity of
257 concentrated proteins and band size. B) Western blotting was carried out to detect the target purified
258 SP-CoV19_{his}-GFP, SP-his_{CoV19}-GFP and negative control SP-*mCov19*_{his} using his antibodies.

259

260 **Figure 3 Competitive ELISA inhibition of ACE2 and RBD binding using anti RBD nanobodies.**
261 Competition binding assays were used to investigate whether the SP-Cov19_{his}-GFP and SP-
262 his_{CoV19}-GFP blocked the binding of RBD to ACE2 compared to the mutant version SP-
263 *mCov19*_{his}. SP-CoV19_{his}-GFP, SP-his_{CoV19}-GFP and SP-*mCov19*_{his} at 1µg/mL and
264 0.1µg/mL were incubated with RBD proteins, both SP-CoV19_{his}-GFP, SP-his_{CoV19}-GFP
265 inhibited RBD bound to ACE-2 but SP-*mCov19*_{his} at 1µg/mL.

266

267 **Supplementary data**

268

269 **Figure S1.** Multiple sequence alignment of protein coding sequences showing the overall structure of
270 the various nanobody constructs. The complementarity determining regions (CDR) 1, 2, and 3, which
271 were mutated in the negative control construct SP-*mCov19*_{his}, are annotated along with other major
272 features.

273 **Figure S2.** A) Western blot serial elution: total of 5ml elution buffer with 500mM imidazole was
274 used to recover of 1mL each sample B) Coomassie blue staining was used to validate purification
275 after Ni-NTA using total protein and purified protein. C) Purified SP-CoV19_{his} samples were
276 pulled together and concentrated using 10Kda size exclusion column to 500µl and tested
277 with competitive ELISA at 100,10,1,0.1 µg/mL.

278

279 **9 References**

280 Asaadi, Y., F. F. Jouneghani, S. Janani and F. Rahbarizadeh (2021). "A comprehensive comparison
281 between camelid nanobodies and single chain variable fragments." *Biomarker Research* **9**(1): 87.

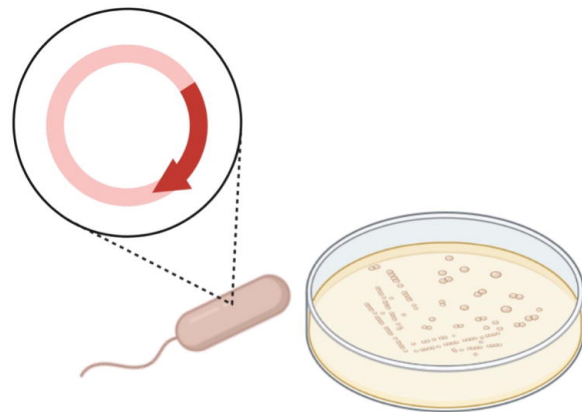
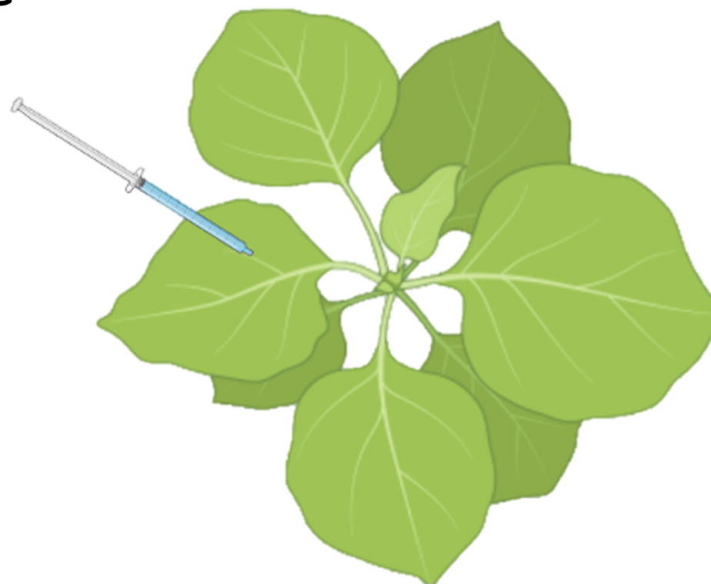
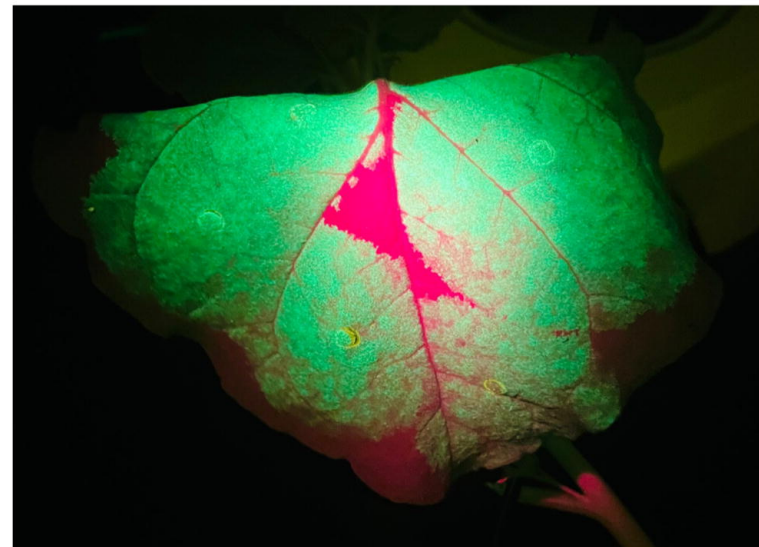
282 Benton, D. J., A. G. Wrobel, P. Xu, C. Roustan, S. R. Martin, P. B. Rosenthal, J. J. Skehel and S. J.
283 Gamblin (2020). "Receptor binding and priming of the spike protein of SARS-CoV-2 for membrane
284 fusion." *Nature* **588**(7837): 327-330.

285 Demone, J., M. Nourimand, M. Maltseva, M. Nasr-Sharif, Y. Galipeau, M.-A. Langlois and A. M.
286 MacLean (2021). "Plant-based production of SARS-CoV-2 antigens for use in a subunit vaccine."
287 [bioRxiv: 2021.2010.2017.464700](https://doi.org/10.1101/2021.2010.2017.464700).

288 Deyev, S. M. and E. N. Lebedenko (2009). "Modern Technologies for Creating Synthetic Antibodies
289 for Clinical application." *Acta Naturae* **1**(1): 32-50.

- 290 Dhama, K., S. Natesan, M. Iqbal Yattoo, S. K. Patel, R. Tiwari, S. K. Saxena and H. Harapan (2020).
291 "Plant-based vaccines and antibodies to combat COVID-19: current status and prospects." Hum
292 Vaccin Immunother **16**(12): 2913-2920.
- 293 Esparza, T. J., N. P. Martin, G. P. Anderson, E. R. Goldman and D. L. Brody (2020). "High affinity
294 nanobodies block SARS-CoV-2 spike receptor binding domain interaction with human angiotensin
295 converting enzyme." Sci Rep **10**(1): 22370.
- 296 Gonzalez-Sapienza, G., M. A. Rossotti and S. Tabares-da Rosa (2017). "Single-Domain Antibodies
297 As Versatile Affinity Reagents for Analytical and Diagnostic Applications." Front Immunol **8**: 977.
- 298 Huang, C., Y. Wang, X. Li, L. Ren, J. Zhao, Y. Hu, L. Zhang, G. Fan, J. Xu, X. Gu, Z. Cheng, T. Yu,
299 J. Xia, Y. Wei, W. Wu, X. Xie, W. Yin, H. Li, M. Liu, Y. Xiao, H. Gao, L. Guo, J. Xie, G. Wang, R.
300 Jiang, Z. Gao, Q. Jin, J. Wang and B. Cao (2020). "Clinical features of patients infected with 2019
301 novel coronavirus in Wuhan, China." Lancet **395**(10223): 497-506.
- 302 Jackson, C. B., M. Farzan, B. Chen and H. Choe (2022). "Mechanisms of SARS-CoV-2 entry into
303 cells." Nature Reviews Molecular Cell Biology **23**(1): 3-20.
- 304 Li, J., S. Lai, G. F. Gao and W. Shi (2021). "The emergence, genomic diversity and global spread of
305 SARS-CoV-2." Nature **600**(7889): 408-418.
- 306 Nishima, W. and M. Kulik (2021). "Full-Length Computational Model of the SARS-CoV-2 Spike
307 Protein and Its Implications for a Viral Membrane Fusion Mechanism." Viruses **13**(6).
- 308 Njeru, F. N. and P. M. Kusolwa (2021). "Nanobodies: their potential for applications in
309 biotechnology, diagnosis and antiviral properties in Africa; focus on application in agriculture."
310 Biotechnology & Biotechnological Equipment **35**(1): 1331-1342.
- 311 Samavati, L. and B. D. Uhal (2020). "ACE2, Much More Than Just a Receptor for SARS-COV-2."
312 Frontiers in Cellular and Infection Microbiology **10**.
- 313 Saxena, S. K., S. Kumar, S. Ansari, J. T. Paweska, V. K. Maurya, A. K. Tripathi and A. S. Abdel-
314 Moneim (2022). "Characterization of the novel SARS-CoV-2 Omicron (B.1.1.529) variant of
315 concern and its global perspective." J Med Virol **94**(4): 1738-1744.
- 316 Wang, Q., Y. Zhang, L. Wu, S. Niu, C. Song, Z. Zhang, G. Lu, C. Qiao, Y. Hu and K.-Y. Yuen
317 (2020). "Structural and functional basis of SARS-CoV-2 entry by using human ACE2." Cell **181**(4):
318 894-904. e899.
- 319 Wang, W., J. Yuan and C. Jiang (2021). "Applications of nanobodies in plant science and
320 biotechnology." Plant Mol Biol **105**(1-2): 43-53.
- 321 Yan, R., Y. Zhang, Y. Li, L. Xia, Y. Guo and Q. Zhou (2020). "Structural basis for the recognition of
322 SARS-CoV-2 by full-length human ACE2." Science **367**(6485): 1444-1448.

323

A**BioXp Gibson Assembly[®]****B****Agrobacterium
transformation****C****Agrobacterium
transient expression****D****UV detection of green
fluorescent protein (GFP)**

Sp-Cov19_his_G

Sp-his_Cov19-G

Sp-mCov19_his

Sp-Cov19_his-G

Sp-his_Cov19-G

Sp-mCov19_his

